ORIGINAL PAPER

Noise-induced collective dynamics in the small-world network of photosensitive neurons

Fan Li[1] · **Xiaola Li[1]** · **Liqing Ren[1]**

Abstract

Photosensitive neurons can capture and convert external optical signals, and then realize the encoding signal. It is confirmed that a variety of firing modes could be induced under optical stimuli. As a result, it is interesting to explore the mode transitions of collective dynamics in the photosensitive neuron network under external stimuli. In this work, the collective dynamics of photosensitive neurons in a small-world network with non-synaptic coupling will be discussed with spatial diversity of noise and uniform noise applied on, respectively. The results prove that a variety of different collective electrical activities could be induced under different conditions. Under spatial diversity of noise applied on, a chimera state could be observed in the evolution, and steady cluster synchronization could be detected in the end; even the nodes in each cluster depend on the degree of each node. Under uniform noise applied on, the complete synchronization window could be observed alternately in the transient process, and steady complete synchronization could be detected finally. The potential mechanism is that continuous energy is pumped in the phototubes, and energy exchange and balance between neurons to form the resonance synchronization in the network with different noise applied on. Furthermore, it is confirmed that the evolution of collective dynamical behaviors in the network depends on the external stimuli on each node. Moreover, the bifurcation analysis for the single neuron model is calculated, and the results confirm that the electrical activities of single neuron are sensitive to different kinds of noise.

Keywords Photosensitive neurons · Non-synaptic coupling · Cluster synchronization · Complete synchronization · Resonance

1 Introduction

The nervous system plays a leading role in regulating the physiological activities in the body and consists of a large number of functional units [1–3]. In the conducted studies, neuron models are used to reproduce the main dynamical characteristics of biological neurons [4–7]. A variety of firing modes (chaotic, quiescent, spiking, and bursting states) have

✉ Fan Li
   lifan0226@126.com

1   College of Energy Engineering, Yulin University, Yulin 719000, People's Republic of China

been confirmed to be induced while the neuron models have different parameters selected or are exposed to different external stimuli [8–13]. For example, the work of Ref. [10] stated that different kinds of electrical activities could be better exhibited in a fractional-order Izhikevich neuron model than in the classical-order model.

The study of the collective dynamical behaviors of coupled neurons has been the focus of much research. In general, the coupled neurons are connected by different kinds of types, such as the chain, small-world, regular network. Then, the collective dynamics between coupled neurons under different conditions are discussed, for example, the feedback control [14], forcing currents, noise [15–18], time delay [19], electromagnetic radiation, electric fields [20], as well as optical and audio signals. It has been proven that the external stimuli could change the membrane potential of neurons, inducing different firing patterns and dynamical behaviors. So far, many excellent works on resonance [21–24], pattern selection [25–28], synchronization and energy estimation [29, 30], chimera states [31, 32], and others have been carried out to explore the potential mechanism behind disease propagation and information encoding. For example, Ref. [19] stated that the dynamical behaviors of asynchrony resonance could be observed under different time delay forms. Wang et al. [20] investigated the effect of the AC electric field on the dynamical activities of the neuron network. Zhang et al. [23] discussed the synchronization between memristive oscillators without direct variable coupling, and declared the mechanism that the resonance could be induced between oscillators due to the energy injection. Hussain et al. [32] studied the collective behavior in a thermosensitive neuron network with non-local coupling; the results confirmed that chimera state could be induced under proper coupling intensity.

With the rise of artificial neural networks (ANNs), the study of intelligent neuron processors is attracting more and more attention, and some neuron models (networks) are modulated and built, since different electrical activities of the neurons could be reproduced by many nonlinear oscillators or circuits with different selected parameters or under periodical stimuli in the dynamical system [33–41]. For example, Ref. [33] reported that the capacitor, memristor, inductor, and resistor could be designed to connect the neurons representing artificial synapses and discussed the collective dynamics. Ref. [35] discussed the learning properties of an online learning system by presenting a differential memristive synapse. Pham et al. [36] studied the dynamics of memristive neural networks and the circuit implementation. Liu and colleagues [37, 38] discussed the synchronization dynamics of the neural circuit connected by a capacitor synapse and a hybrid synapse realized by a resistor and an induction coil, respectively.

In fact, it is necessary and meaningful to consider the physical effect when building the neural network, such that the electromagnetic induction could be induced in the cell due to the change in the concentration of charged ions. It has been shown that different kinds of transitions could be induced under electromagnetic radiation [42–48]. Based on these results, some other neuron models were proposed to describe the dynamical behaviors while applying different external stimuli. In the work of Ref. [49], a kind of photosensitive neuron model is proposed to show the effect of light stimulus on the firing modes of the neuron system. In this neuron model, a phototube is introduced to convert the light stimuli into electric signals, and it is proven that the quiescent, spiking, bursting, and even chaotic behaviors could be activated by the photocell, which is consistent with the main characteristics of biological neurons.

It should be emphasized that most studies about the synchronization between neurons are coupled by direct variable. In Ref. [23], the resonance synchronization is discussed while the memristive chaotic oscillators is coupled without variable coupling. It is because the energy could be pumped and exchanged between coupling channels, and then the

energy flow between the nonlinear oscillators could be balanced. In fact, the photosensitive neuron model is similar to the memristive chaotic oscillators. As a result, it is very interesting to explore the synchronization and firing patterns between coupled photosensitive neuron models without direct variable coupling.

In this paper, the collective behaviors of coupled photosensitive neuron models distributed in the small-world network with non-synaptic coupling are discussed. Due to the sensitivity of photosensitive neuron to external stimuli, the work is carried out by two ways:(1) the spatial diversity of noise applied on; (2) the uniform noise applied on. Furthermore, bifurcation analyses for single neuron and two statistical synchronization parameters are calculated to show the evolution of the synchronization degree.

2 Model and schemes

The revised Fitzhugh-Nagumo (FHN) neuron model is called a photosensitive neuron model [49], since a phototube is designed into the neuron model as a voltage source. The neuron model is described as

$$
\begin{cases}
\frac{dx}{dt} = x(1 - \varsigma) - \frac{1}{3}x^3 - y + u_s \\
\frac{dy}{dt} = c(x + a - by)
\end{cases}
\tag{1}
$$

where x is the fast variable representing the membrane potential, y is the recovery variable, and a, b, c, and ζ are parameters.

$$
u_s = A \cos \omega t
\tag{2}
$$

where u_s is a time-varying voltage source, which is converted from light by the phototube, A denotes the amplitude, and ω is the frequency of the excitation signal.

It is confirmed in Ref. [49] that a variety of dynamical behaviors of neurons could be induced with different parameters selected. As a result, it is interesting to explore the evolution of collective dynamical behaviors of coupled neurons distributed in a small-world network just external stimuli are imposed on. In this work, a kind of non-synaptic coupling between neurons is applied while the photosensitive neurons are exposed to spatial diversity of noise and uniform noise, respectively.

The dynamical equations for photosensitive neuron models are distributed in a small-world network with non-synaptic coupling under spatial diversity of noise applied on, which are shown as:

$$
\begin{cases}
\frac{dx_i}{dt} = x_i(1 - \varsigma) - \frac{1}{3}x_i^3 - y_i + u_s + \sum_{j=1}^{N} A_{ij}\xi(t) \quad i,j = 1, \ldots, N \\
\frac{dy_i}{dt} = c\left(x_i + a - by_i\right)
\end{cases}
\tag{3}
$$

where N denotes the number of nodes and i and j represent the node position in the network. The symbol $\xi(t)$ indicates the Gaussian white noise; its statistical properties are described as $\langle \xi(t) \rangle = 0$, $\langle \xi(t)\xi(s) \rangle = 2k\delta(t - s)$ and k is the noise intensity [50]. A_{ij} represents the adjacency matrix and $A_{ij} = 1$ indicates that the two nodes are connected, otherwise $A_{ij} = 0$.

As shown in Eq. (3), the non-synaptic coupling between neurons with spatial diversity of noise is actually described by the degree of each node in the network (i.e., the network structure). As a result, it is interesting to explore the collective dynamics between photosensitive neurons with non-synaptic coupling while the uniform noise is applied on; the corresponding dynamical equations are as follows:

$$\begin{cases} \frac{dx_i}{dt} = x_i(1-\varsigma) - \frac{1}{3}x_i^3 - y_i + A\cos\omega t + e^{g\sum_{j=1}^{N}A_{ij}\xi(t)} \Big/ d(i) \quad i,j = 1,\dots,N \\ \frac{dy_i}{dt} = c(x_i + a - by_i) \end{cases} \tag{4}$$

where $d(i)$ is the degree of the node i in the network and g denotes the noise strength. Furthermore, the statistical parameter is calculated to show the synchronization degree of the collective dynamical behaviors in the network [51]; the formula is as follows:

$$R = \frac{\langle F^2 \rangle - \langle F \rangle^2}{\frac{1}{N}\sum_{i=1}^{N}\left(\langle x_i^2 \rangle - \langle x_i \rangle^2\right)}$$

$$F = \frac{1}{N}\sum_{i=1}^{N}x_i \tag{5}$$

where x_i represents a variable of node j and N denotes the total number of nodes in the network. A value of $R \approx 1$ indicates a perfect synchronization, while $R \approx 0$ shows that the detected synchronization is not perfect.

In order to intuitively depict the synchronization degree, another statistical parameter of the synchronization error is defined and calculated as follows:

$$E = \frac{1}{T}\int_{t_0}^{t_0+T}\sum_{j=2}^{N}|(x(1) - x(j))| \tag{6}$$

where T is the transient time and the symbol $|*|$ represents the absolute value. A value of $E \approx 0$ indicates that a complete synchronization is detected; otherwise, an incomplete synchronization is detected.

3 Results and discussion

In the simulation, we used the fourth-order Runge–Kutta algorithm for the calculation and time step $h = 0.01$. It has been confirmed that the photosensitive neuron model could show different kinds of firing modes (spiking, bursting, and even chaotic states) by activating the photocell [49].

3.1 Bifurcation analysis for the single neuron model

In order to discuss the collective dynamical behaviors in the network, the dynamic characteristic for a single neuron model exposed to the noise is discussed at first.

In fact, the physiological activities in the body could show different electrical activities while the body is exposed to different external stimuli, for example, cold environment, hot environment, and so on. As a result, it is meaning to study the evolution of dynamical behaviors while the single neuron is exposed to different external environment. As reported in Ref. [50], the noise could be generated as negative or positive values randomly. Here, the generated different noise represents different kinds of external environment.

As a result, the bifurcation data for the single neuron exposed to different noise are calculated, and the results are shown in Fig. 1.

The results in Fig. 1 show the bifurcation analysis for a single neuron model with the increase of noise strength k while different noise is induced. It is confirmed that a variety of dynamical behaviors could be observed while the neuron is exposed to different noise. It is found in Fig. 1(a, b) ((c, d)) that the larger value of generated noise could promote the evolution of dynamical behavior. Moreover, compared with the results in Fig. 1(a, c) ((b, d)), it is proven that the negative noise benefits to promote the evolution of dynamical behaviors of electrical activities. In a word, these results state that the electrical activities of neuron are sensitive to different kinds of noise.

Furthermore, the corresponding time series of membrane potential x of single neuron are plotted to give the results, which are tracked in Fig. 2.

The results in Fig. 2(a–d) show the time series of membrane potential x of single neuron under different conditions. It is proven that different kinds of electrical activities could be
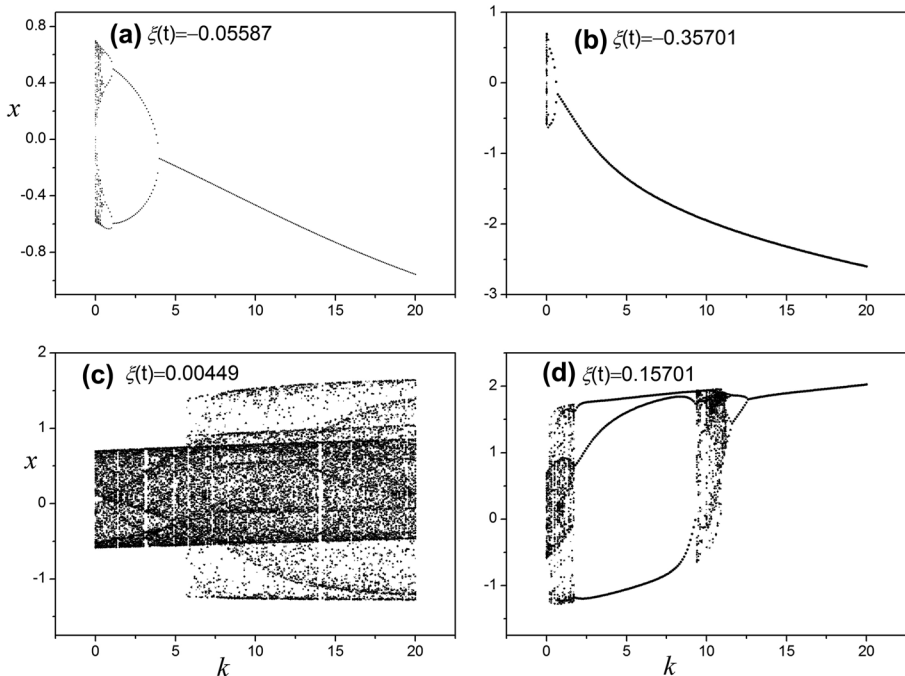

Fig. 1 Bifurcation diagram for single neuron with different noise strength k while the neuron is exposed to different kinds of noise. The generated noise (**a**) $\xi(t)=-0.05587$; (**b**) $\xi(t)=-0.35701$; (**c**) $\xi(t)=0.00449$; (**d**) $\xi(t)=0.15701$. It is proven that different evolution of dynamical behaviors of single neuron could be induced under different external stimulus
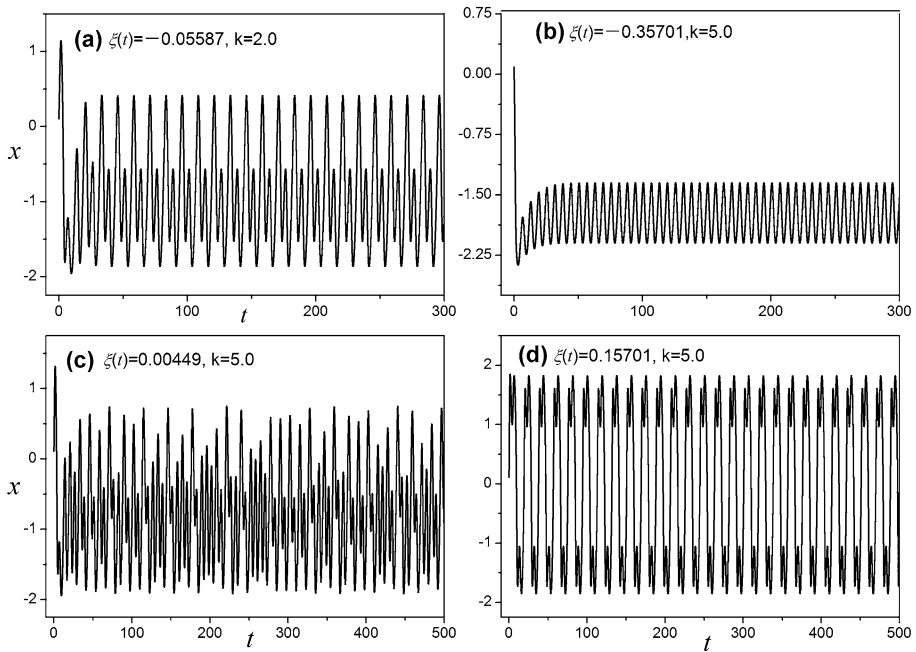
Fig. 2 Time series of membrane potential x of the neuron model under different condition; the generated noise and noise strength are (**a**) $\xi(t)=-0.05587$, $k=2.0$; (**b**) $\xi(t)=-0.35701$, $k=5.0$; (**c**) $\xi(t)=0.00449$, $k=5.0$; (**d**) $\xi(t)=0.15701$, $k=5.0$. These results confirm the result in Fig. 1

induced under different external stimuli. In a word, the results in Figs. 1 and 2 state that the photosensitive neuron is sensitive to different kinds of external stimuli. As a result, it is interesting to explore the collective dynamical behaviors in the network while the media exposed to external stimuli.

In the network, the state of the single photosensitive neuron model is set in chaotic state, and the parameters are selected as $a=0.7$, $b=0.8$, $c=0.1$, $\zeta=0.175$, $A=0.9$, and $\omega=1.004$. The corresponding phase diagram of the single neuron in a chaotic state is shown in Fig. 3.

Fig. 3 The phase diagram of the single photosensitive neuron model with the parameters $a=0.7$, $b=0.8$, $c=0.1$, $\zeta=0.175$, $A=0.9$, and $\omega=1.004$. The single neuron model is chaotic state
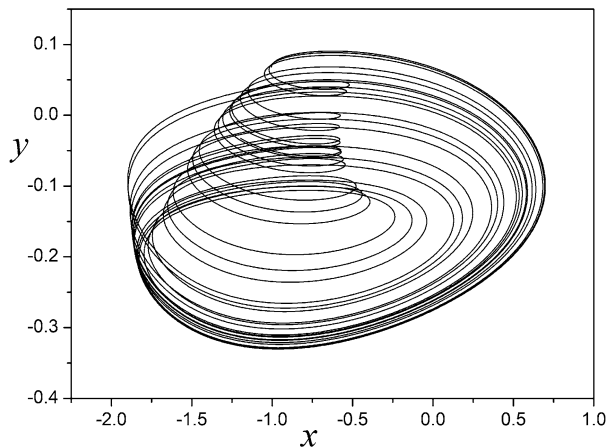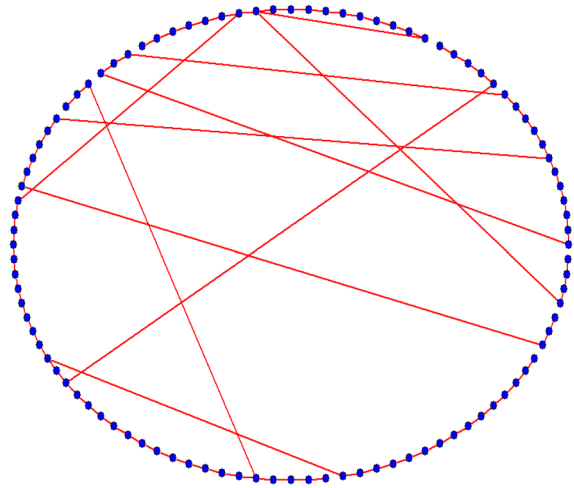
The results in Fig. 3 indicate that the chaotic state of each node in the network is detected with the selected parameters. Based on these results, the collective dynamics in the small-world network will be discussed, while the neurons connected with non-synaptic coupling (no direct variable coupling). The work will be carried by two ways: (1) neurons with non-synaptic coupling under spatial diversity of noise applied on; (2) neurons with non-synaptic coupling under uniform noise applied on.

The network has the following parameters: the number of nodes $N=100$, rewiring probability $p=0.1$, and average degree $d=2$. The schematic diagram for the network is shown in Fig. 4. Interestingly, the degree distribution of all the nodes could be from the structure of the small-world network, which is shown in Fig. 5. It could be observed that there are four cluster nodes: $d=1$, $d=2$, $d=3$, and $d=4$. The nodes with $d=2$ form the biggest cluster, and there is a single node with $d=4$.
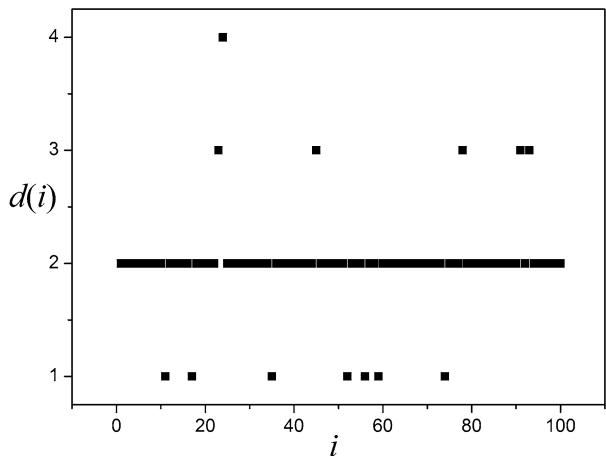
3.2 Non-synaptic coupling with spatial diversity of noise

In this section, the discussion about the collective response of light-sensitive neurons without synaptic coupling is carried out, while the external noise with distributed distribution is considered. The time series of the membrane potential and attractor for the sampled nodes are calculated, and two statistical parameters are calculated to depict the evolution of collective dynamics while selecting different noise strength k values. The corresponding results are shown in Figs. 6, 7, 8, 9, 10, 11, 12 and 13.

First, the synchronization parameter R and synchronization error E are separately calculated with different selected values of noise strength k.

A large simulation data confirm that there are five different evolution stages that could be found in the evolution of R and E in Fig. 6, which are S_0 ($k \leq 0.1$), S_1 ($0.1 < k < 1.8$), S_2 ($1.8 \leq k < 2.75$), S_3 ($2.75 \leq k \leq 3.3$), and S_4 ($k > 3.3$). Interestingly, it is confirmed that R cannot increase to 1, and E cannot decrease to 0, which means that the complete synchronization cannot be detected in the network. As a result, it is interesting to explore what transitions are formed at the different stages. We respectively calculated the time series and attractor for the sampled nodes with different noise strength k values to show the mode transitions of the collective dynamical behaviors in these five stages.

At first, a variety of calculation confirmed that all the nodes are in chaotic states while selecting the noise strength k in the S_0 area. In the following, the time series and attractor for some sampled nodes are calculated to show the transitions of the collective dynamics while selecting the noise strength k in S_1, S_2, S_2, and S_4.

Given a selection of k values in the S_1 area, the phase diagrams for different sampled nodes with different degrees in the network are calculated. The results are plotted in Fig. 7.

Figure 7 shows that in some clusters, the nodes show a periodic state ($d = 2$, 3, and 4, respectively). However, the nodes with $d = 1$ are in a chaotic state. As a result, the periodic and chaotic states could coexist in the network under a proper noise strength k. Furthermore, it is interesting to find that partial synchronization could be observed in the clusters in which the nodes are in a periodic state. The time series of the sampled nodes are tracked in Fig. 8, which shows that partial synchronization could be detected in the clusters in which the nodes show periodic electrical activities.
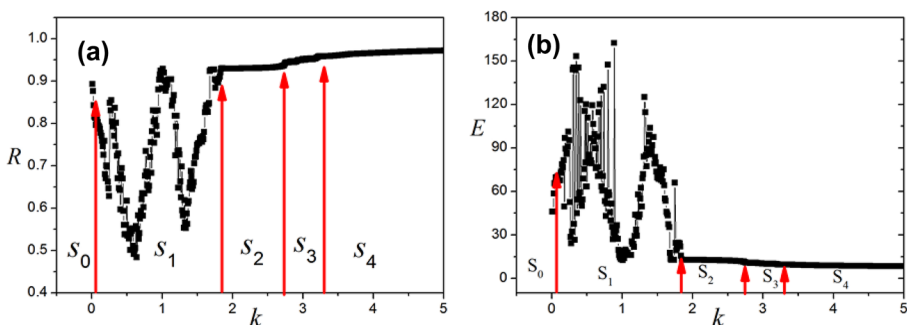

Fig. 6 The evolution of the synchronization parameter R and synchronization error E with the increase of the noise strength k. This confirms that different evolution stages could be observed
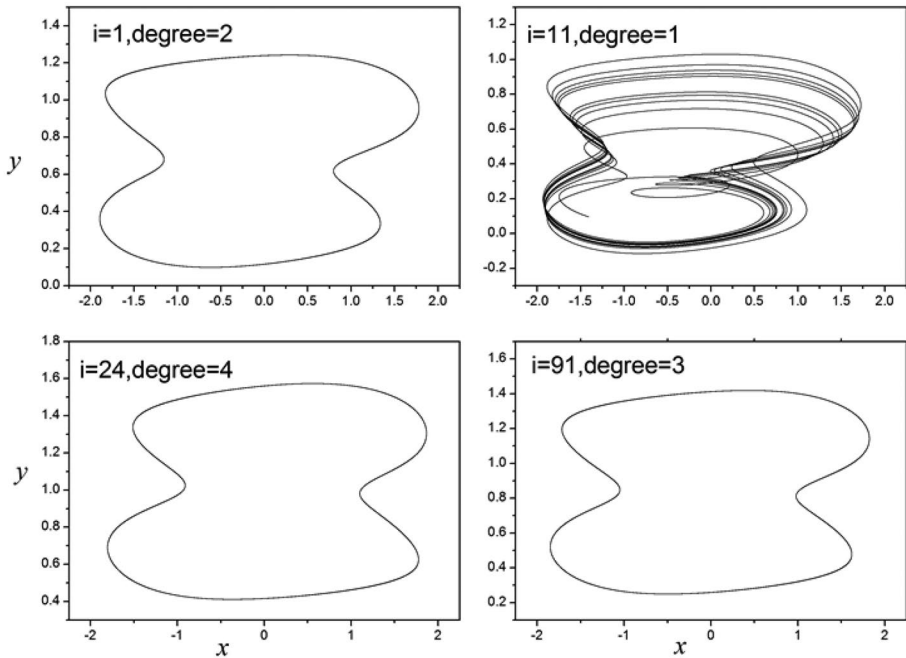
Fig. 7 The attractors of the sampled nodes selected in different clusters in the network, with the noise strength $k=0.5$ being selected in the area S_1. The coexistence of chaotic and periodic states is observed in the network

Moreover, it is interesting to find that there are a variety of dynamical behaviors that could be observed with a stronger noise strength selected in the S_1 area. The corresponding results are shown in Fig. 9.

Compared with the results in Fig. 7, the results in Fig. 9 show that some different dynamical behaviors could be found in some clusters. Specifically, it is found that the states of some nodes have some interesting changes, from chaotic to periodic in the nodes with $d=1$, and from periodic to chaotic in the nodes with $d=3$, with a noise
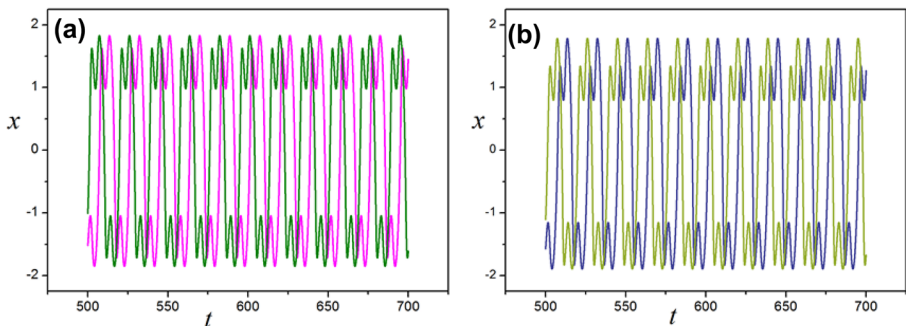

Fig. 8 The time series of the nodes selected in different clusters in the network with **a** $d=3$, **b** $d=2$, and $k=0.5$ selected in the area S_1. Partial synchronization could be detected in the cluster
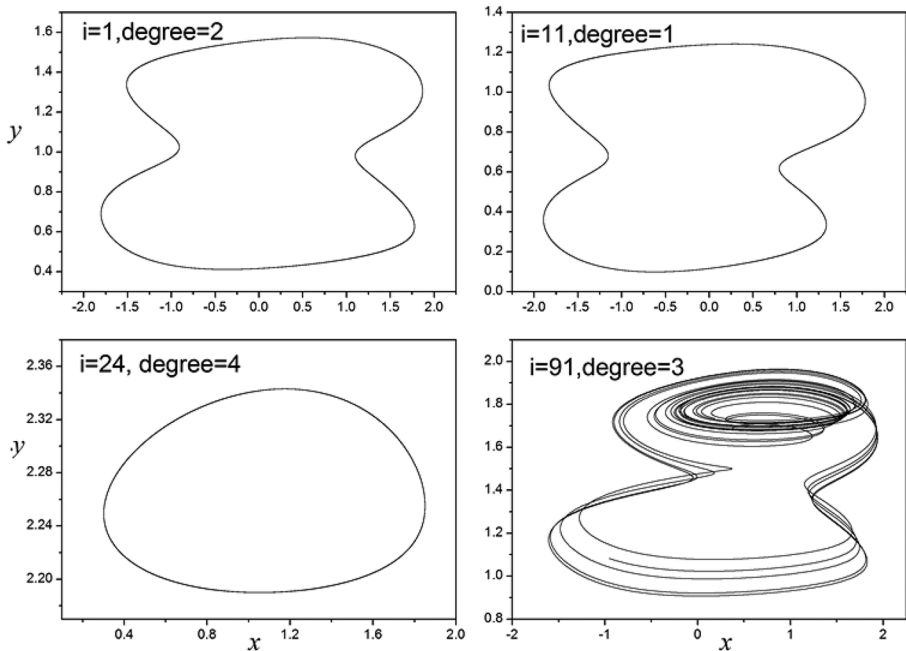
🍎 Springer

Fig. 9 The attractor for the sampled nodes selected in different clusters in the network, while selecting a noise strength $k=1.0$ in the area S_1. The coexistence of chaotic and periodic states is observed in the network and the states of nodes show instability, which could be from chaotic to periodic ($d=1$) or from periodic to chaotic ($d=3$) compared with the results in Fig. 6

strength $k=1.0$. That is to say the injected energy in each neuron is unstable under this noise.

In addition, it is interesting to find that cluster synchronization could be realized in the cluster nodes. The time series for the sampled nodes are plotted in Fig. 10, which shows that the periodic and chaotic states could also coexist in the network with different noise strength values selected in the S_1 area. However, the nodes in the cluster (plotted in Fig. 10(d), with degree $=2$) realize the complete synchronization. As a result, cluster synchronization could be realized in a cluster with a proper noise strength, and the noise coupling could promote the synchronization. It means that the synchronization state and non-synchronization state coexist in the network. That is to say the chimera state could be induced in the network under spatial diversity of noise applied on with proper noise intensity.

A significant part of the simulation results proves that chaotic and periodic states coexist in the network, and the states of nodes in any cluster could change while selecting different k values, even state of the network could become from asynchrony to chimera state when the increase of noise strength selected in the S_1 area.

As we continue to increase the noise strength by selecting k in the S_2 area, different results could be detected. The time series and attractor for the sampled nodes are plotted in Fig. 11. It is confirmed in Fig. 11(a) that all the nodes in different clusters realize the cluster synchronization, which means that the nodes in each cluster with the same degrees achieve complete synchronization. Furthermore, Fig. 11(b) shows that all the nodes are in
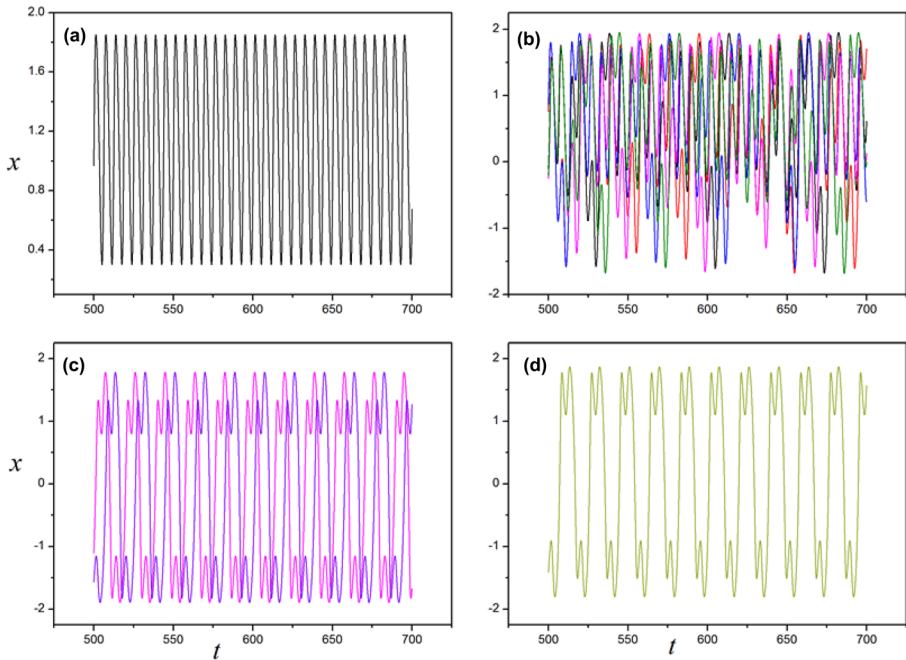
Fig. 10 The time series for the nodes in different clusters in the network with **a** $d=4$, **b** $d=3$, **c** $d=1$, **d** $d=2$, and $k=1.0$ selected in the area S_1. Chaotic and periodic states coexist, and cluster synchronization could be detected in the cluster nodes in the network. Chimera state is induced in the network under proper noise strength and noise promotes the realization of synchronization

periodic states. A large part of the simulation results states that the cluster synchronization could be detected in the S_2 area.

Based on the above-mentioned results, we continue to have a selection of k in the S_3 area, and different results could still be found. The corresponding time series for the nodes with different degrees are calculated and shown in Fig. 12, which shows that the nodes with degree $=1$ lose synchronization compared with the results in Fig. 11.
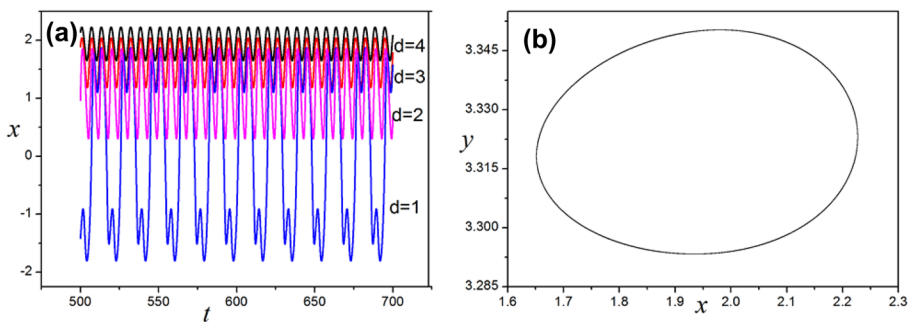

Fig. 11 a The time series of the nodes in the network and **b** the attractor for the sampled node, with $i=1$ and $k=2.0$ in the area S_2. All the clusters realize the cluster synchronization, and all the nodes are in periodic states
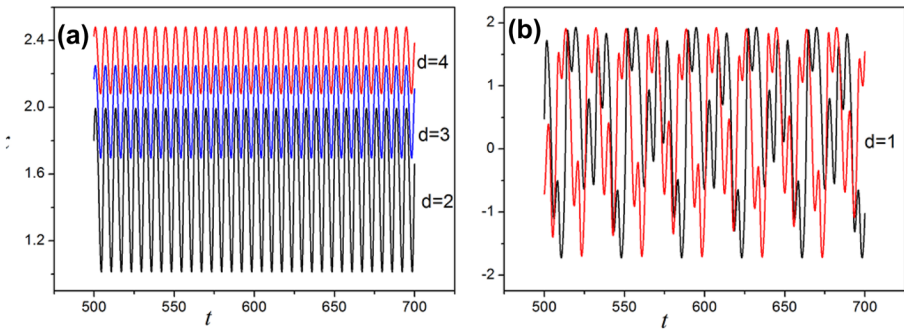
Fig. 12 The time series for the sampled nodes with different degrees and $k=2.75$ in the area S_3. A coexistence of chaotic and periodic states could be detected in the network, and more clusters realize the complete synchronization compared with the results in the area S_1. Chimera state is induced in the S_3 area again

Furthermore, it is found that these nodes change from periodic to chaotic states, but the nodes in other clusters keep the cluster synchronization and stay in periodic states. It means that the chimera state could be induced in the S_3 area again.

A significant part of the simulation results confirms that only the nodes with degree $=1$ lose the synchronization and keep chaotic states in the S_3 stage. The reason is that continuous energy is pumped in the phototubes in the network, and then energy exchange and balance between neurons due to the resonance in the network. The chimera state is induced under the external stimuli because the energy between neurons is unstable.

We continue to increase the noise strength k and make a selection in the S_4 stage, which shows that all the clusters realize the cluster synchronization again. The corresponding time series are plotted in Fig. 13, which shows that cluster synchronization could be detected in the network, and the nodes in different clusters have different amplitudes, which are related to the degree of each node. Further calculation results prove that the steady cluster synchronization could be observed even when a stronger noise strength is selected. It means that the energy pumping and exchange between neurons in the network are in stable state under the resonance.
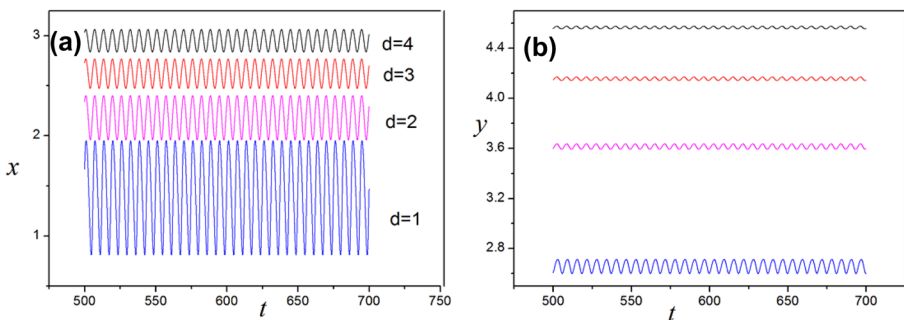

Fig. 13 The time series of x and y for all the nodes with different degrees and $k=5.0$. It is confirmed that all the nodes in the different clusters in the network achieve cluster synchronization

In summary, we proved that a variety of mode transitions of the dynamical behaviors could be detected, and four cluster nodes realize the cluster synchronization, in the end, while the coupling between neurons is realized by non-synaptic coupling with spatial diversity of noise applied. Notably, the distribution of the nodes in each cluster is related to the degree of each node. Furthermore, we proved that a variety of mode transitions could be detected, which are from asynchrony to chimera to cluster synchronization to chimera to stable cluster synchronization in the end with the increase of noise strength k. The mechanism is that continuous energy could be pumped in the phototubes, and energy exchange and balance between neurons to form the resonance in the network with different noise strength values. That is to say the different kinds of mode transitions induced in the network due to the different degree of energy resonance exchange between neurons in the transient process. In fact, these results confirmed that the collective dynamical behaviors in the network are dependent on the network connection under the spatial diversity of noise applied on.

3.3 Non-synaptic coupling with uniform noise

In this section, we will discuss what mode transitions of collective dynamics could be detected, while the neurons connected by non-synaptic coupling with uniform noise applied on. The corresponding dynamical equation is shown in Eq. (4).

First, the synchronization parameter R and synchronization error E are calculated while selecting different noise strength g values. The results are shown in Fig. 14.

It is interesting to see there are some different results observed in Fig. 14 compared with the results in Fig. 6. The parameter R could reach 1 and the E could decrease to 0, which means that complete synchronization could be detected in the network ($R \approx 1$, $E \approx 0$). Furthermore, it is found that the evolution of the collective dynamical behaviors could be divided into six stages: S_0 ($g \leq 0.3$), S_1 ($0.4 \leq g \leq 1.91$), S_2 ($1.92 \leq g \leq 2.28$), S_3 ($2.29 \leq g \leq 3.39$), S_4 ($3.4 \leq g \leq 3.46$), S_5 ($3.47 \leq g \leq 3.68$), and S_6 ($g \geq 3.69$).

From the results plotted in Fig. 14, it is found that several complete synchronization windows could be observed in the evolution process. As a result, it is interesting to explore what mode transitions of collective dynamics are shown in the whole evolution. The time series and attractor for the sampled nodes in the network are calculated, and the results are plotted in Figs. 15, 16 and 17.
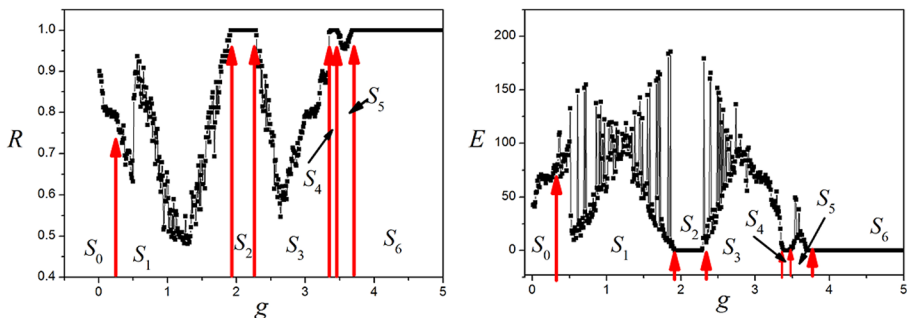

Fig. 14 Evolution of the order parameter R and synchronization error E with different noise strength g values
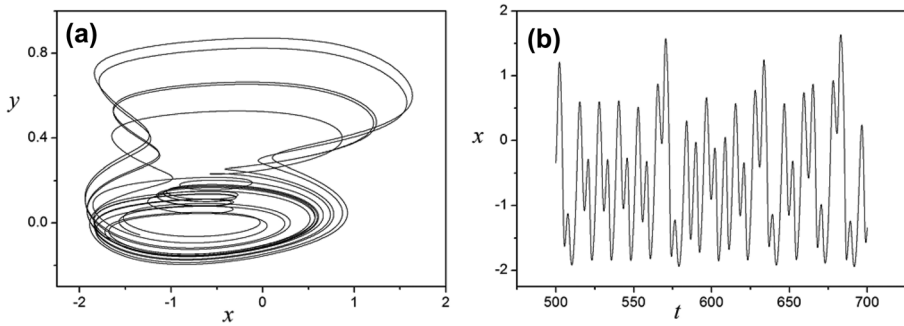
Fig. 15 The attractor and time series for the sampled nodes in the network, with $i=1$ and $k=0.3$. All the nodes are in chaotic states and no synchronization could be detected

First, the time series and attractor for the sampled nodes are calculated with a small g in the S_0 area, and the results are shown in Fig. 15.

The results in Fig. 15 prove that there is no synchronization, and all the nodes are in chaotic states. Next, we increase the coupling strength and select the noise strength g in the areas S_1, S_3, and S_5, respectively. The results are shown in Fig. 16.

It is interesting to observe in Fig. 16 that all the nodes in the network are in periodic states and form two clusters, which realize cluster synchronization, respectively. Furthermore, it

Fig. 16 The time series for all the nodes in the network with different noise strength g values: (**a**) $g=0.7$, (**b**) $g=2.6$, and (**c**) $g=3.6$; (**d**) the attractor of the sampled node with $i=1$ and $g=3.6$. The nodes form two clusters, which realize cluster synchronization, and all the nodes are in periodic states. The nodes in each cluster are random and change with different coupling strength g values
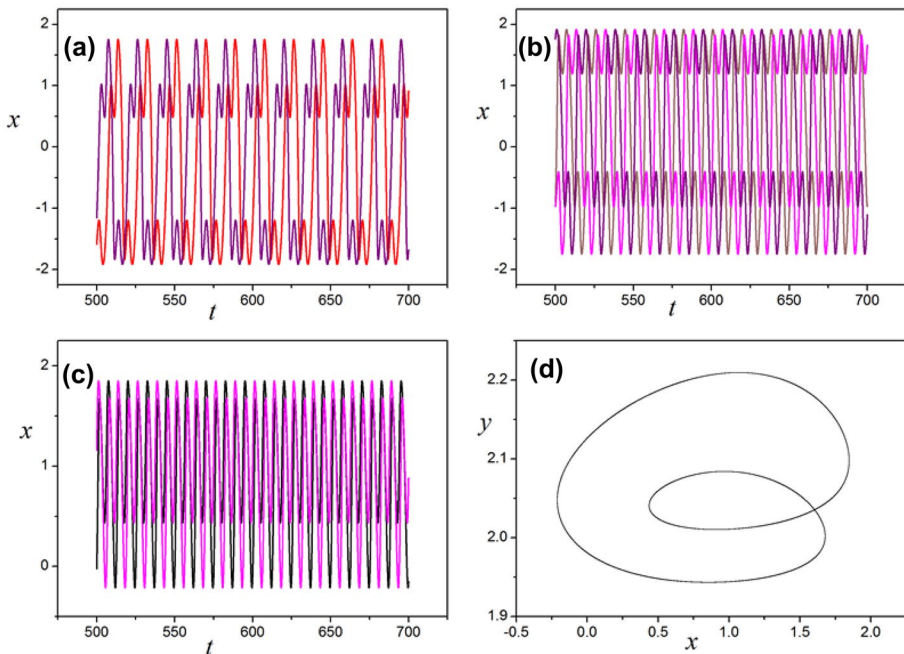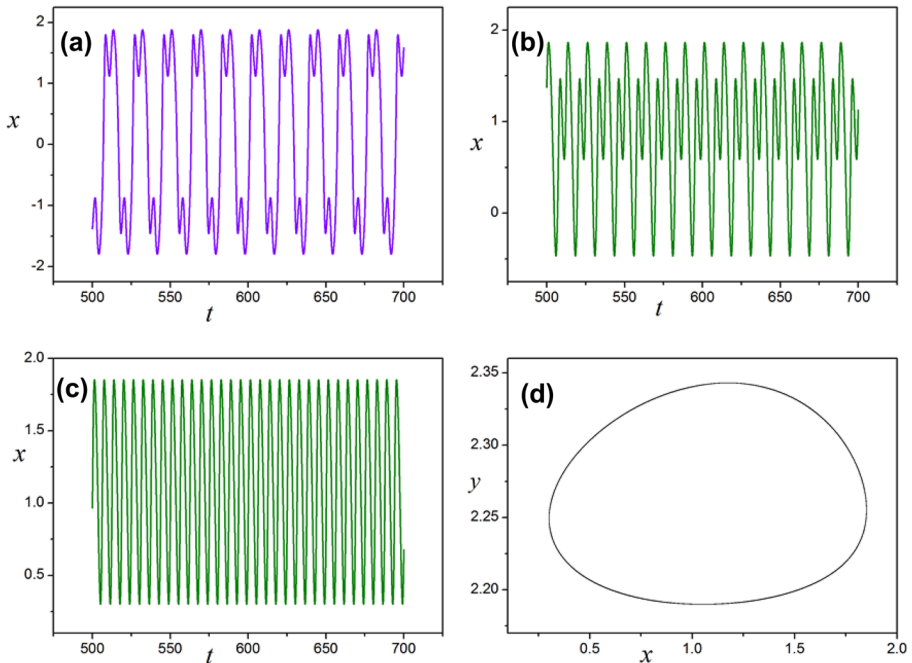
Fig. 17 The time series for all the nodes in the network with different noise strength g values: (**a**) $g=2.1$, (**b**) $g=3.42$, and (**c**) $g=4.0$; (**d**) the attractor of the sampled node with $i=1$ and $g=4.0$. Complete synchronization is detected in the different synchronization areas and all the nodes are in periodic states

should be emphasized that the nodes in each cluster are random and change with different values of the noise strength g. Besides, the distribution of the nodes between the two clusters is independent of the degree of each node. This explains why there are large fluctuations in the evolution of two order parameters with different coupling strength g values.

Next, we carry out similar simulations, by calculating the time series and attractor while having a selection of noise strength g values in the areas S_2, S_4, and S_6. The results are plotted in Fig. 17, which proves that complete synchronization could be observed, and shows different dynamical behaviors in different synchronization areas, with all the nodes being in periodic states. A number of simulation results confirm that steady complete synchronization could be observed in the S_6 area, which means that complete synchronization could still be detected with a stronger noise strength g.

In summary, compared to the results with spatial diversity of noise applied on, some difference could be observed, which is the steady complete synchronization could be detected in the end with uniform noise applied on. Furthermore, it could be confirmed that the areas of S_2, S_4, and S_6 are complete synchronization areas, while S_1, S_3, and S_5 are cluster synchronization areas. It means that the cluster synchronization and complete synchronization alternate in the process of evolution, before the stable complete synchronization is achieved finally. Moreover, in the cluster synchronization area, it is noted that all the nodes form two clusters, which realize the cluster synchronization, respectively. It is noted that the nodes in each cluster are random and their distribution between the clusters is not related to structure, and even the number of the nodes in the cluster changes with the noise strength g.

The potential mechanism is that the continuous pumped energy exchange and balance between neurons, and then the resonance synchronization is induced in the network under proper noise strength values. However, the realization of complete synchronization in the end is because the energy uniformity is achieved at each point under the resonance due to uniform noise applied on. In the process of synchronization, the pumped energy in each node is unstable and changeable under the effect of resonance with different noise strength selected. That is why cluster synchronization and complete synchronization appear alternately. Furthermore, the results prove that the network connection has not contributed to the collective behavior in the network under uniform noise applied on.

4 Conclusion

In this study, we investigate the mode transitions of collective dynamical behaviors of photosensitive neurons distributed in the small-world network with non-synaptic coupling under different external stimuli. In the simulation, the results are discussed with spatial diversity of noise and uniform noise applied on, respectively. It is proven that a variety of interesting dynamics could be detected in the network under different conditions.

Under the spatial diversity of noise, it is confirmed that the chimera state could be detected in the evolution, and the steady cluster synchronization could be realized finally. Furthermore, it is found that the distribution of the nodes in each cluster is related to the degree of each node. The mechanism is that continuous energy could be pumped in the phototubes, then energy exchange and balance between neurons to form the resonance synchronization in the network with different noise strength selected. Moreover, the energy of each node depends on the spatial diversity of noise (the structure of the network).

Under uniform noise, cluster synchronization and complete synchronization appear alternately in the evolution, and steady complete synchronization is detected finally. Furthermore, it is confirmed the nodes in each cluster change are random and do not depend on the structure of the network. The potential mechanism is also that the pumped energy exchange and balance between neurons to form the resonance synchronization, but each node could keep uniform energy in the end due to resonance under uniform noise applied on. That is why the steady complete synchronization is detected.

In a word, these results declare that different kinds of collective dynamical behaviors could be induced in the photosensitive neuron network with non-synaptic coupling due to the resonance. The results could provide some information for neurodynamics and applying in biology and neural circuits. Furthermore, it is very interesting to have a study on the energy estimation of the evolution of collective behaviors in the network.

Declarations

Ethical approval The study is purely theoretical and does not involve any experiment with animals that would require ethical approval.

Informed consent The study does not involve any participants that would have to give their informed consent.

Conflict of interest The authors declare no competing interests.

References

1. Churchland, M.M., Cunningham, J.P., Kaufman, M.T., Foster, J.D., Shenoy, K.V.: Neural population dynamics during reaching. Nature **487**, 51–56 (2012)
2. Kotaleski, J.H., Blackwell, K.T.: Modelling the molecular mechanisms of synaptic plasticity using systems biology approaches. Nat. Rev. Neurosci. **11**, 239–251 (2010)
3. Stent, G.S.: Semantics and neural development. In: Sharma, C.S. (ed.) Organizing Principles of Neural Development. pp. 145–160. Springer (1984)
4. Chay, T.R.: Chaos in a three-variable model of an excitable cell. Physica D **16**, 233–242 (1985)
5. Tsumoto, K., Kitajima, H., Yoshinaga, T., Aihara, K., Kawakami, H.: Bifurcations in Morris-Lecar neuron model. Neurocomputing **69**(4–6), 293–316 (2006)
6. González-Miranda, J.M.: Complex bifurcation structures in the Hindmarsh-Rose neuron model. Int. J Bifurcat. Chaos **17**(9), 3071–3083 (2007)
7. Izhikevich, E.M.: Dynamical Systems in Neuroscience: The Geometry of Excitability and Bursting. The MIT Press, Cambridge (2007)
8. Gu, H.G., Pan, B.B.: A four-dimensional neuronal model to describe the complex nonlinear dynamics observed in the firing patterns of a sciatic nerve chronic constriction injury model. Nonlinear Dyn. **81**(4), 2107–2126 (2015)
9. Gu, H.G., Pan, B.B., Li, Y.Y.: The dependence of synchronization transition processes of coupled neurons with coexisting spiking and bursting on the control parameter, initial value, and attraction domain. Nonlinear Dyn. **82**(3), 1191–1210 (2015)
10. Mondal, A., Upadhyay, R.K.: Diverse neuronal responses of a fractional-order Izhikevich model: journey from chattering to fast spiking. Nonlinear Dyn. **91**(2), 1275–1288 (2018)
11. Lee, S.G., Kim, S.: Parameter dependence of stochastic resonance in the stochastic Hodgkin-Huxley neuron. Phys. Rev. E **60**, 826–830 (1999)
12. Wang, H.T., Sun, Y.J., Li, Y.C., Chen, Y.: Influence of autapse on mode-locking structure of a Hodgkin-Huxley neuron under sinusoidal stimulus. J. Theoret. Biol. **358**, 25–30 (2014)
13. Hauschildt, B., Janson, N.B., Balanov, A., Schoell, E.: Noise-induced cooperative dynamics and its control in coupled neuron models. Phys. Rev. E **74**(5), 051906 (2006)
14. Ma, J., Song, X.L., Tang, J., Wang, C.N.: Wave emitting and propagation induced by autapse in a forward feedback neuronal network. Neurocomputing **167**, 378–389 (2015)
15. Ma, J., Wu, Y., Ying, H., Jia, Y.: Channel noise-induced phase transition of spiral wave in networks of Hodgkin-Huxley neurons. Chin. Sci. Bull. **56**, 151–157 (2011)
16. Yang, J., Zhou, W.N., Shi, P., Yang, X.Q., Zhou, X.H., Su, H.Y.: Adaptive synchronization of delayed Markovian switching neural networks with Levy noise. Neurocomputing **156**, 231–238 (2015)
17. García-Ojalvo, J., Schimansky-Geier, L.: Noise-induced spiral dynamics in excitable media. Europhys. Lett. **47**, 298–303 (1999)
18. Upadhyay, R.K., Mondal, A., Teka, W.W.: Mixed mode oscillations and synchronous activity in noise induced modified Morris-Lecar neural system. Int. J. Bifurcat. Chaos **27**(5), 1730019 (2017)
19. Yu, W.T., Tang, J., Ma, J., Yang, X.Q.: Heterogeneous delay-induced asynchrony and resonance in a small-world neuronal network system. Europhys. Lett. **114**, 50006 (2016)
20. Wang, H.T., Chen, Y.: Spatiotemporal activities of neural network exposed to external electric fields. Nonlinear Dyn. **85**, 881–891 (2016)
21. Yao, Y.G., Yi, M., Hou, D.J.: Coherence resonance induced by cross-correlated Sine-Wiener noises in the FitzHugh–Nagumo neurons. Int. J. Mod. Phys. B **31**, 1750204 (2017)
22. Wang, Q., Zhang, H., Perc, M., Chen, G.R.: Multiple firing coherence resonances in excitatory and inhibitory coupled neurons. Commun. Nonlinear Sci. Numerm. Simul. **17**, 3979–3988 (2012)
23. Zhang, Y., Zhou, P., Yao, Z., Ma, J.: Resonance synchronisation between memristive oscillators and network without variable coupling. J. Phys. **95**, 49 (2021)
24. Yilmaz, E., Ozer, M., Baysal, V., Perc, M.: Autapse-induced multiple coherence resonance in single neurons and neuronal networks. Sci. Rep. **6**, 30914 (2016)
25. Zhao, H.Y., Huang, X.X., Zhang, X.B.: Turing instability and pattern formation of neural networks with reaction–diffusion terms. Nonlinear Dyn. **76**, 115 (2014)
26. Ma, J., Qin, H.X., Song, X.L., Chu, R.T.: Pattern selection in neuronal network driven by electric autapses with diversity in time delays. Int. J. Mod. Phys. B **29**, 1450239 (2015)

27. Sharma, S.K., Mondal, A., Mondal, A., Upadhyay, R.K., Ma, J.: Synchronization and pattern formation in a memristive diffusive neuron model. Int. J. Bifurcat. Chaos **31**(11), 2130030 (2021)

28. Xu, Y., Wang, C.N., Lv, M., Tang, J.: Local pacing, noise induced ordered wave in a 2D lattice of neurons. Neurocomputing **207**, 398–407 (2016)

29. Wu, F.Q., Ma, J., Zhang, G.: Energy estimation and coupling synchronization between biophysical neurons. Sci. China Tech. Sci. **63**(4), 625–636 (2020)

30. Sun, X.J., Li, G.F.: Synchronization transitions induced by partial time delay in a excitatory–inhibitory coupled neuronal network. Nonlinear Dyn. **89**, 2509–2520 (2017)

31. Majhi, S., Bera, B.K., Ghosh, D., Perc, M.: Chimera states in neuronal networks: a review. Phys. Life Rev. **28**, 100–121 (2019)

32. Hussain, I., Ghosh, D., Jafari, S.: Chimera states in a thermosensitive FitzHugh-Nagumo neuronal network. Appl. Math. Comput. **410**, 126461 (2021)

33. Ma, J., Tang, J.: A review for dynamics in neuron and neuronal network. Nonlinear Dyn. **89**, 1569–1578 (2017)

34. Xu, F., Zhang, J.Q., Fang, T.T., Huang, S.F., Wang, M.S.: Synchronous dynamics in neural system coupled with memristive synapse. Nonlinear Dyn. **92**, 1395–1402 (2018)

35. Nair, M.V., Muller, L.K., Indiveri, G.: A differential memristive synapse circuit for on-line learning in neuromorphic computing systems. Nano Futures **1**, 035003 (2017)

36. Pham, V.T., Jafari, S., Vaidyanathan, S., Volos, C., Wang, X.: A novel memristive neural network with hidden attractors and its circuitry implementation. Sci. China Technol. Sci. **59**, 358–363 (2016)

37. Liu, Z.L., Wang, C.N., Zhang, G., Zhang, Y.: Synchronization between neural circuits connected by hybrid synapse. Int. J. Mod. Phys. B **33**(16), 1950170 (2019)

38. Liu, Z.L., Wang, C.N., Jin, W.Y., Ma, J.: Capacitor coupling induces synchronization between neural circuits. Nonlinear Dyn. **97**, 2661–2673 (2019)

39. Rajagopal, K., Bayani, A., Khalaf, A.J.M., Namazi, K., Jafari, S.: A no-equilibrium memristive system with four-wing hyperchaotic attractor. AEU-Int. J. Electron. Commun. **95**, 207–215 (2018)

40. Ma, S.Y., Yao, Z., Zhang, Y., Ma, J.: Phase synchronization and lock between memristive circuits under field coupling. AEU-Int. J. Electron. Commun. **105**, 177–185 (2019)

41. Zhang, J.H., Liao, X.F.: Synchronization and chaos in coupled memristor-based FitzHugh-Nagumo circuits with memristor synapse. AEU-Int. J. Electron. Commun. **75**, 82–90 (2017)

42. Lv, M., Ma, J.: Multiple modes of electrical activities in a new neuron model under electromagnetic radiation. Neurocomputing **205**, 375–381 (2016)

43. Duan, L.X., Cao, Q.Y., Wang, Z.J., Su, J.Z.: Dynamics of neurons in the pre-Bötzinger complex under magnetic flow effect. Nonlinear Dyn. **94**(3), 1961–1971 (2018)

44. Meng, F.Q., Zeng, X.Q., Wang, Z.L.: Dynamical behavior and synchronization in time-delay fractional-order coupled neurons under electromagnetic radiation. Nonlinear Dyn. **95**(2), 1615–1625 (2019)

45. Takembo, C.N., Mvogo, A., Fouda, H.P.E., Kofane, T.C.: Effect of electromagnetic radiation on the dynamics of spatiotemporal patterns in memristor-based neuronal network. Nonlinear Dyn. **95**(2), 1067–1078 (2019)

46. Takembo, C.N., Mvogo, A., Fouda, H.P.E., Kofane, T.C.: Wave pattern stability of neurons coupled by memristive electromagnetic induction. Nonlinear Dyn. **96**(2), 1083–1093 (2019)

47. Guo, S.L., Xu, Y., Wang, C.N., Jin, W.Y., Hobiny, A., Ma, J.: Collective response, synapse coupling and field coupling in neuronal network. Chaos Solitons Fractals **105**, 120–127 (2017)

48. Panahi, S., Rostami, Z., Rajagopal, K., Namazi, H., Jafari, S.: Complete dynamical analysis of myocardial cell exposed to magnetic flux. Chin. J. Phys. **64**, 363–373 (2020)

49. Liu, Y., Xu, W.J., Ma, J., Alzahrani, F., Hobiny, A.: A new photosensitive neuron model and its dynamics. Front. Inform. Technol. Electron. Eng. **21**, 1387–1396 (2020)

50. Fox, R.F., Gatland, I.R., Roy, R., Vemuri, G.: Fast, accurate algorithm for numerical simulation of exponentially correlated colored noise. Phys. Rev. A **38**(11), 5938–5940 (1988)

51. Xu, C., Gao, J., Sun, Y.T., Huang, X.: Explosive or continuous: incoherent state determines the route to synchronization. Sci. Rep. **5**, 12039 (2015)

Publisher's Note Springer Nature remains neutral with regard to jurisdictional claims in published maps and institutional affiliations.